

A Myxoid Fibrotic Reaction Pattern is Associated with Metastatic Risk in Cutaneous Squamous Cell Carcinoma

Eugenia HERNÁNDEZ-RUIZ^{1,2#}, Inmaculada HERNÁNDEZ-MUÑOZ^{3#}, Emili MASFERRER⁴, Carla FERRÁNDIZ-PULIDO², Evelyn ANDRADES³, Javier GIMENO⁵, Xavier DURAN⁶, Vicente GARCÍA-PATOS², Ramon M. PUJOL¹ and Agusti TOLL¹

Departments of ¹Dermatology and ⁵Pathology, Hospital del Mar, Parc de Salut Mar, ²Department of Dermatology, Hospital Universitari Vall d'Hebron, Departament de Medicina de la UAB, Universitat Autònoma de Barcelona, ³Group of Inflammatory and Neoplastic Dermatological Diseases and ⁶Methodological and biostatistical advisory service, IMIM (Hospital del Mar Medical Research Institute), and ⁴Department of Dermatology, Hospital Universitari Mútua de Terrassa, Barcelona, Spain

[#]Both authors contributed equally to this work.

Although desmoplasia has been associated with poor prognoses in cutaneous squamous cell carcinoma, little attention has been paid to the patterns of fibrosis. This study aimed to examine the different stromal fibrotic patterns as markers of metastatic risk. We performed a multicenter retrospective study that included 102 cutaneous squamous cell carcinomas (52 non-metastatic and 50 metastatic carcinomas). Clinical and histopathological data were registered. The fibrotic reaction pattern was classified as mature, intermediate or immature depending on the presence of keloid-like collagen and myxoid stroma. The immature pattern (areas characterized by myxoid changes with no inflammation) was observed in 18 samples and its presence was significantly associated with immunosuppression, budding, desmoplasia, perineural invasion, anatomic level, tumoural depth and metastatic risk in the multivariate analysis. Our findings suggest that the presence of an immature myxoid fibrotic pattern, which can be easily identified by routine hematoxylin-eosin staining, is strongly associated with metastatic risk.

Key words: metastasis; fibrosis; cutaneous squamous cell carcinoma.

Accepted Aug 31, 2018; Epub ahead of print Sep 3, 2018

Acta Derm Venereol 2019; 99: 89–94.

Corr: Agustí Toll, Department of Dermatology, Hospital del Mar, Parc de Salut Mar, Universitat Autònoma de Barcelona, ES-08003 Barcelona, Spain. E-mail: atoll@parcdesalutmar.cat, atoll@clinic.cat

Metastatic cutaneous squamous cell carcinomas (MSCCs) usually involve the regional lymph nodes, and occur in approximately 4–5% of patients (1). Active research in cutaneous SCC (cSCC) is aimed at the identification of prognostic markers of clinical value that could help identify those patients at higher metastatic risk. Prominent clinical factors linked to an aggressive clinical behaviour and metastatic risk include tumoural size, immunosuppression and certain tumour locations such as the ears, lips and areas of chronic injury. Some histological parameters of the primary tumour, including depth, poor histological differentiation and perineural invasion have also been associated with poor prognosis (2–4).

Epithelial to mesenchymal transition (EMT), a mechanism by which epithelial cells lose adhesion and

SIGNIFICANCE

Cutaneous squamous cell carcinomas are the second most frequent non-melanoma skin cancers. Despite their generally good prognosis, approximately 2–5% metastasize, usually to regional lymph nodes. Recent works have elucidated the relevance of the tumour microenvironment, consisting of a stromal reaction, a vascular and lymphatic network and the presence of specific inflammatory cell subpopulations, in the development of metastases. In this study we have characterized different types of stromal reaction patterns in cutaneous squamous cell carcinoma, including desmoplasia, and have found that the presence of a myxoid peritumoral infiltration, easily recognisable by hematoxylin eosin stains, is associated with an increased metastatic risk.

acquire mesenchymal traits that allow them to invade and disseminate (5), has been shown to be involved in the metastasis of a variety of epithelial tumours. Indeed, we have previously reported that the presence of EMT markers is associated with an increased metastatic risk in cSCC (6). Tumour budding, pathologically characterized by clusters or single tumoural cells that may reflect cells undergoing EMT, has also been recently linked to nodal metastasis in cSCC (7, 8).

The EMT process can be induced by the tumoural microenvironment through the release of cytokines and extracellular matrix proteins by cancer-associated fibroblasts (CAFs). In addition to their effect on epithelial tumoural cells, CAFs may also generate a fibrotic stroma. The role of the fibrotic reaction in cancer development and progression remains controversial. While some studies suggest that the host may favour a desmoplastic response to limit tumour aggressiveness (9), others have shown that the fibrotic stroma induced by CAFs might benefit the tumour by inhibiting access to immune cells (10–13). In this sense, the association between desmoplastic reaction and poor outcome has been observed in several cancers such as cholangiocarcinoma, breast, pulmonary, pancreatic, tongue, rectal and colorectal carcinomas (11, 14–18). cSCC with a desmoplastic phenotype, characterized by strands and nests of tumour cells surrounded by a prominent fibrous stromal response, may also pose an increased risk of

recurrence and metastases (3, 19). Indeed, the presence of desmoplasia is considered to be a high-risk factor by the NCCN and the European Dermatology Forum, the European Association of Dermato-Oncology, and the European Organization for Research and Treatment of Cancer (EDF-EADO-EORTC) guidelines (20, 21). Unlike other carcinomas, such as rectal and colorectal cancers (17, 18), little attention has been given to the study of fibrotic patterns and their correlation with biological behaviour in cSCC. In this study, we aimed to study the association between different fibrotic patterns and lymphatic metastatic risk in cSCC.

PATIENTS AND METHODS

Patients

Cutaneous biopsies from patients presenting cSCC from 3 tertiary hospitals in Spain between 2001 to 2011 were included in the study. Selected biopsies corresponded either to primary cSCC tumours of patients who had developed metastatic spread (MSCC) or to cSCC without an aggressive clinical behaviour after a long follow-up period (NMSCC). Fifty primary MSCC with lymph node ($n=40$) and/or cutaneous in-transit metastases ($n=10$) were included in the study. Additionally, 52 cutaneous SCCs that had not developed metastatic spread after at least a 5-year follow-up period (NMSCC) were also evaluated as a control group.

A set of clinical data were retrospectively collected from each patient including sex, age, immunosuppression status and cause of immunosuppression, year of diagnosis, recurrences, tumour size and location. TNM staging evaluation by two systems (AJCC-8 and Brigham and Women's Hospital – BWH) (22, 23) was recorded from each patient.

Ethics approval was obtained from all the participating centers, in accordance with the guidelines of the Helsinki Declaration of 1975, as revised in 1983.

Histologic parameters

Following a systematized protocol, the following histopathological data were evaluated in all samples in H&E-stained glass slides: thickness (in mm), level of invasion, degree of differentiation (well, moderate, poor), presence of vascular or perineural invasion and, when present, the diameter of the affected nerve (in mm).

Tumoural budding and fibrotic stroma were simultaneously evaluated by two of the authors (AT and MEH), who were blind to the aggressiveness of the tumours.

Fibrotic stroma. Desmoplasia was defined as the presence of small tumoural nests surrounded by stromal fibrosis in at least one third of the tumoural sample.

The fibrotic reaction pattern (FRP) was evaluated at the advancing edge of the tumour by H&E and classified into one of 3 categories (mature, intermediate, or immature) as previously reported (18), depending on the presence of keloid-like collagen and myxoid stroma. Keloid-like collagen was defined as the presence of bundles of hypocellular collagen and bright eosinophilic hyalinization. Myxoid stroma showed an amorphous stromal substance with an extracellular amphophilic or basophilic material. The presence of a myxoid or keloidal stroma was considered when observed with the 40x objective lens in areas with scarce or no inflammatory infiltrate.

FRP was considered mature (mFR) when the fibrotic stroma lacked a keloid-like collagen or myxoid stroma and contained mature collagen fibres stratified into an onion-like pattern (Fig. 1).

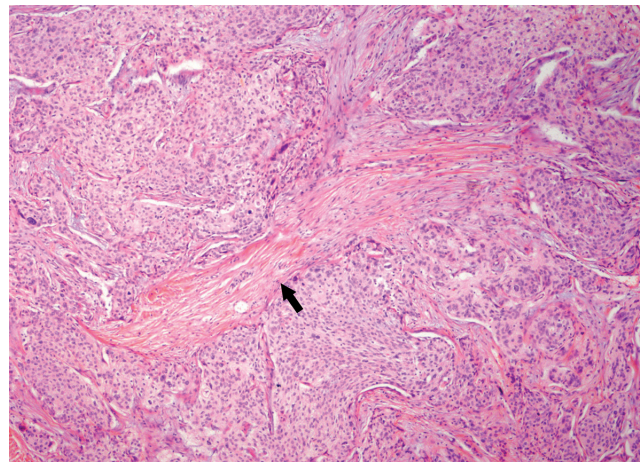


Fig. 1. Mature fibrotic reaction pattern (arrow) (H&E 40x).

Intermediate fibrotic reaction was designated for tumours showing keloid-like fibrosis intermingled in mature stroma, while immature fibrosis (iFR) was assigned to tumours showing areas of myxoid changes with or without keloidal fibrosis (Fig. 2). The more immature fibrotic areas were considered for analysis.

A quantitative evaluation of the FRP was also performed. The area of fibrosis (percentage) surrounding the advancing edge of the tumour was recorded. The width of the fibrotic reaction was also categorised from 0 to 3 as follows: 1: 0–100 μm ; 2: 100–200 μm ; 3: > 200 μm . A fibrosis burden score (area x width: 0–300) for fibrosis was calculated.

Tumour budding. Tumour budding was defined based on the number of foci of isolated cancer cells or on the presence of a cluster comprising < 5 cells in the invasive frontal region, as previously reported (24). Cases with 5 or more foci, identified using a 40x objective lens, were regarded as positive for budding.

Stainings and immunohistochemistry. Alcian blue stainings were performed in cases showing a myxoid pattern in the H&E stain, in order to detect mucin deposition. To this end, slides were deparaffinized and hydrated. They then were stained with Alcian blue solution (1% Alcian Blue in 3% acetic acid solution, pH 2.5) for 30 min and rinsed with water. Slides were counterstained with hematoxylin for 5 min, dehydrated and mounted with DPX.

For immunohistochemistry, slides were deparaffinized, hydrated and antigen retrieval was performed in 10 mM citrate (pH 6) for 10 min in a pressure cooker (for α -SMA) or with Proteinase K 15 min at 37°C (for fibronectin). Tissues were then quenched for

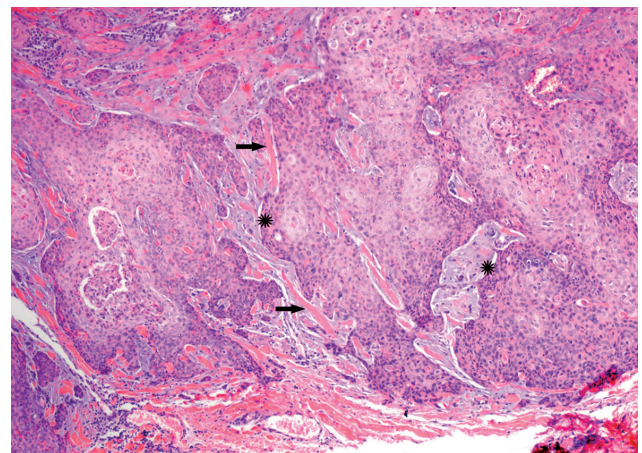


Fig. 2. Immature fibrotic reaction pattern with myxoid (asterisks) and keloidal areas (arrow) (H&E 40x).

endogenous peroxidase activity with 4% (vol/vol) H₂O₂ for 10 min at room temperature, blocked and incubated with primary antibodies overnight at 4°C. After washing, Envision+System-HRP antibody reagent was applied Dako (Agilent Technologies). Immunohistochemical reactions were developed using diaminobenzidine (DAB) as a chromogenic substrate. Sections were counterstained with hematoxylin, dehydrated and mounted. The following antibodies were used: α -SMA from Sigma (A2547) and Fibronectin from Dako (A0245).

Statistical analyses

Correlations between categorical variables were evaluated using χ^2 test or Fisher's exact test when appropriate. Continuous data were compared using a Student's *t*-test if the sample distribution was normal, or otherwise via a Mann-Whitney *U*-test.

A multivariate logistic regression analysis was performed to determine which clinico-pathological features were predictive of lymphatic metastases. $p < 0.05$ was considered statistically significant. Analysis was conducted with SPSS 18.0 (SPSS Inc., Chicago, IL, USA).

RESULTS

Biopsy specimens ($n = 102$) from a total number of 102 patients were included in the study (Table I). Fifty patients presented MSCC, 40 of them to the regional lymph-nodes and 10 showing cutaneous in-transit satellitosis.

More than half of the patients were men (69.6%), and the median age was 79 years (Q1: 72; Q3: 85). Most of the cSCC were excised from sun-exposed areas, mainly the head and neck (85 cSCC), followed by extremities (14 cSCC) and trunk (3 cases). Twelve patients were immunosuppressed (8 kidney recipients, 1 hepatic recipient, 1 Crohn's disease, 1 chronic lymphatic leukemia and 1 patient undertaking mycophenolate to treat glomerulonephritis). Twelve cases involved recurrences.

In the whole data set, 36 patients had mFR whereas 18 had iFR. Only 3 cases showed an intermediate fibrotic pattern. Recurrent cSCC presented mFR and iFR equally.

Budding was observed in 34 of 50 MSCC (68%) and 18 of 52 NMSCC (34.6%; $p < 0.01$). The iFR pattern

Table I. Clinical and histopathological variables. Univariate analysis for metastatic risk

	NMSCC ($n = 52$)	MSCC ($n = 50$)	<i>p</i>
<i>Clinical variables, n (%)</i>			
<i>Area</i>			
Head	42 (80.8)	43 (86)	NS
Trunk	1 (1.9)	2 (4)	
Extremities	9 (17.3)	5 (10)	
Sun exposure, Yes	47 (94)	45 (90)	NS
Horizontal size > 20 mm	20 (38.5)	19 (41.3)	NS
Recurrent case, Yes	2 (3.8)	10 (20.4)	0.013
Immunosuppression, Yes	6 (11.5)	6 (13)	NS
<i>Pathological variables</i>			
<i>Differentiation, n (%)</i>			
Good	21 (40.4)	7 (14)	< 0.01
Moderate	28 (53.8)	35 (70)	
Poor	3 (5.8)	8 (16)	
Tumour thickness > 6 mm, n (%)	10 (19.2)	22 (47.8)	< 0.01
Clark level ≥ 4 , n (%)	35 (67.3)	44 (93.6)	< 0.01
Perineural invasion, Yes, n (%)	1 (1.9)	8 (16)	0.015
Nerve diameter ≥ 0.1 mm, n (%)	0 (0)	7 (14)	< 0.01
Vascular invasion, Yes, n (%)	0 (0)	2 (4)	NS
Desmoplasia, Yes, n (%)	1 (1.9)	3 (6)	NS
Budding, Yes, n (%)	18 (34.6)	34 (68)	< 0.01
Mature fibrosis, n (%)	18 (34.6)	18 (36)	NS
Intermediate fibrosis pattern, Yes, n (%)	0 (0)	3 (6)	NS
Myxoid fibrosis, Yes, n (%)	2 (3.8)	16 (32)	< 0.01
Fibrosis burden, median (IQR)	0 (0;135)	40 (0;160)	0.036
<i>Staging systems, n (%)</i>			
<i>TNM (AJCC-8)</i>			
pT1	25 (48.1)	12 (25.5)	< 0.01
pT2	14 (26.9)	6 (12.8)	
pT3	13 (25)	26 (55.3)	
pT4	0 (0)	3 (6.4)	
<i>TNM (Brigham)</i>			
1	25 (48.1)	10 (21.7)	< 0.01
2a	23 (44.2)	23 (50)	
2b	4 (7.7)	9 (19.6)	
3	0 (0)	4 (8.7)	

NMSCC: Nonmetastatic cutaneous squamous cell carcinoma; MSCC: Metastatic cutaneous squamous cell carcinoma; IQR: interquartile range.

was observed in 16 of 50 MSCC (32%) and in 2 of 52 NMSCC (3.8%; $p < 0.01$). Unlike mFR, iFR was mostly observed in isolated foci and in surrounding budding areas (Figs 3a and 4).

Although iFR mostly surrounded the budding areas (89% of the cases with myxoid changes), only 30.7% of tumours with budding had an associated iFR pattern. Interestingly, while budding showed a sensitivity superior

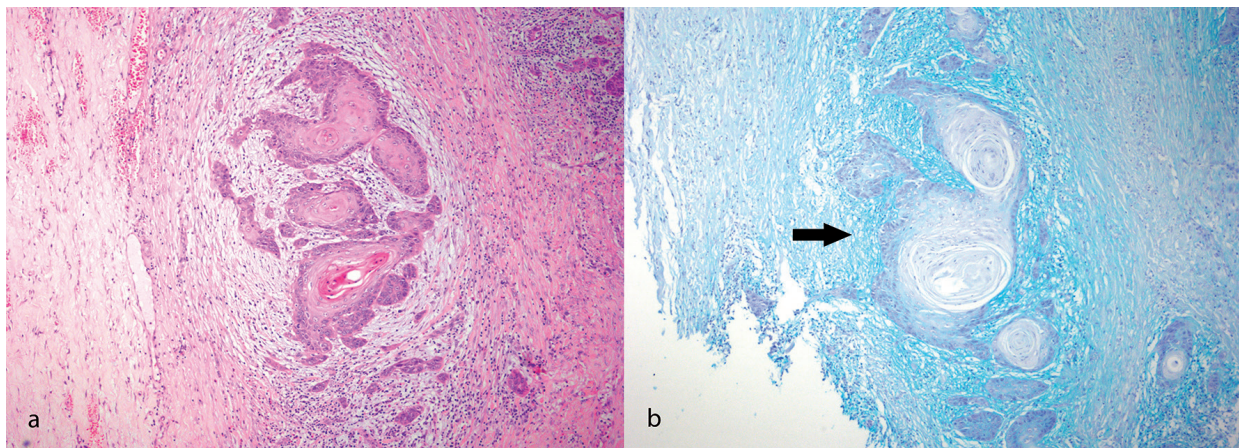


Fig. 3. a) Immature fibrotic reaction pattern with myxoid peritumoral areas segregating an inflammatory infiltrate (H&E 40x). b) Alcian blue showing a larger stain around the tumour (arrow) (40x).

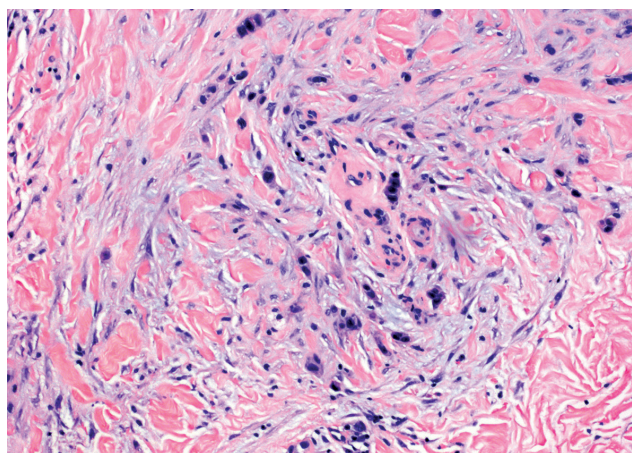


Fig. 4. Immature fibrotic reaction pattern surrounding an area of tumoral budding. H&E 40x.

to iFR in predicting aggressiveness (68% vs 32%), iFR showed a better specificity (96.2% vs 65.4%).

In an attempt to better characterize the stromal fibroblasts, we carried out α -SMA staining, though positivity was only detected in 2 cases with iFR (**Fig. 5**). In contrast, increased expression of mucopolysaccharides (stained with Alcian blue) and fibronectin was frequently observed in areas with a myxoid reaction pattern, although this was not restricted only to this pattern (data not shown) (Fig. 3b).

Univariate analysis (Table I) revealed that previous recurrence, anatomic level (Clark ≥ 4), tumour thickness, budding, histological differentiation, myxoid stroma, peritumoural fibrosis burden and perineural invasion (and nerve diameter > 0.1) were significantly associated with metastasis development. Conversely, age, vascular invasion, desmoplasia and tumour size were not significantly associated with metastatic risk. Both the AJCC and Brigham's staging systems adequately classified both the MSCC and NMSCC groups, although the later proved to be more accurate.

Multivariate analysis, adjusted by age and sex, revealed that the myxoid stroma was the only independent factor associated with lymphatic metastases, with an odds

Table II. Univariate and multivariate analyses for metastatic risk

	Univariate analysis			Multivariate analysis		
	OR _{row}	CI 95%	<i>p</i>	OR _{adj}	CI 95%	<i>p</i>
<i>Clinical variables</i>						
Area	0.77	0.43–1.36	0.37			
Sun exposure	0.57	0.13–2.55	0.47			
Horizontal size > 2 cm	1.13	0.50–2.53	0.77	1.42	0.93–2.17	0.10
Recurrent case	6.41	1.33–30.96	0.02	3.88	0.38–39.42	0.25
Immunosuppression	1.15	0.34–3.85	0.82			
<i>Pathological variables</i>						
Differentiation	3.10	1.47–6.57	0.003	2.38	0.84–6.70	0.10
Tumour thickness ≥ 6 mm	3.85	1.57–9.47	0.003	1.03	0.88–1.22	0.71
Clark level ≥ 4	7.12	1.93–26.28	0.003	2.55	0.49–13.22	0.26
Perineural invasion	9.71	1.17–80.82	0.035	6.45	0.39–107.49	0.19
Desmoplasia	3.26	0.33–32.39	0.31			
Budding	4.01	1.76–9.15	0.001	2.77	0.68–11.3	0.16
Myxoid fibrosis	11.77	2.54–54.50	0.002	13.81	1.70–112.02	0.014
Fibrosis burden score	1.01	1.00–1.01	0.05	0.99	0.98–1.00	1.10
<i>Staging systems</i>						
TNM (AJCC-8)	2.23	1.06–4.68	0.034			
TNM (Brigham)	2	1.24–3.22	0.004			

OR: odds ratio; CI: confidence interval; adj: adjusted. Bold: significant value.

ratio of 13.81 (95% confidence interval 1.70–112.01) (**Table II**). This pattern was associated with immunosuppression, budding, desmoplasia, perineural invasion, anatomic level (Clark ≥ 4) and tumoural depth (**Table III**).

DISCUSSION

Analysis of fibrosis in cSCC has attracted little attention in the literature, with the exception of desmoplasia. This is in striking contrast with the widely reported association between fibrosis and poor prognosis in several cancers (11, 14–18, 25, 26). Fibrosis in cancer is induced by cancer-associated fibroblasts (CAFs) or myofibroblasts, which can induce EMT and cancer cell migration (27, 28). Peritumoural fibrosis may favour tumoural progression by several mechanisms: driving integrin-dependent cell adhesion and migration, regulating tumour plasticity or by impairing tumour immunosurveillance.

In the present work, we observed an association between fibrosis burden and metastatic risk in the uni-

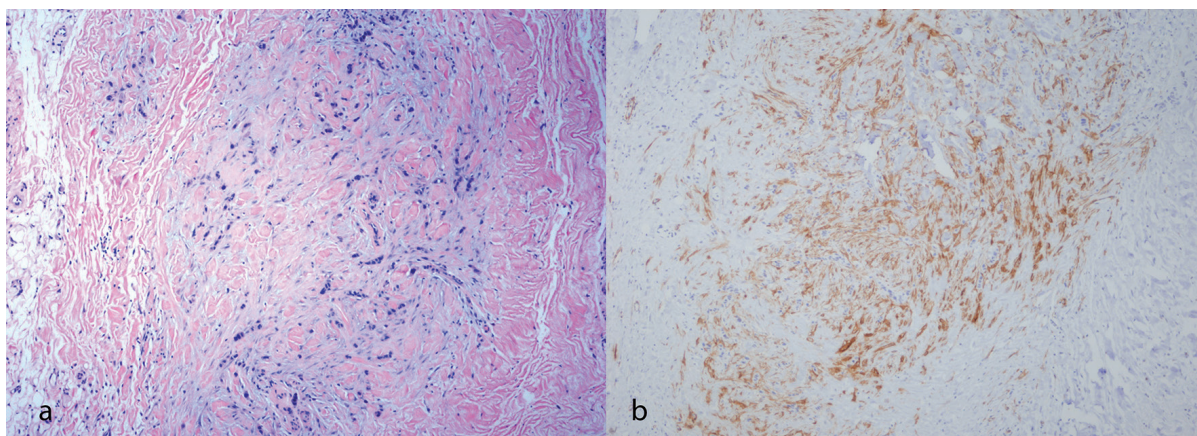


Fig. 5. a) Cutaneous squamous cell carcinoma with a myxoid reaction (H&E 40x) and b) α -SMA-expressing cells.

Table III. Univariate analysis for the presence of myxoid fibrosis

	Myxoid fibrosis		p
	Absence	Presence	
<i>Clinical variables, n (%)</i>			
Total	84 (82.3)	18 (17.6)	
<i>Area</i>			
Head	70 (83.3)	15 (83.3)	NS
Trunk	2 (2.4)	1 (5.6)	
Extremities	12 (14.3)	2 (11.1)	
Sun exposure, Yes	76 (92.7)	16 (88.9)	NS
Horizontal size >20 mm	31 (38.8)	8 (44.4)	NS
Recurrent case, Yes	8 (9.5)	4 (23.5)	NS
Immunosuppression, Yes	7 (8.5)	5 (31.2)	<0.01
<i>Pathological variables</i>			
<i>Differentiation, n (%)</i>			
Good	26 (31)	2 (11.1)	NS
Moderate	50 (59.5)	13 (72.2)	
Poor	8 (9.5)	3 (16.7)	
Tumour thickness, >6 mm, n (%)	23 (28)	9 (56.3)	0.041
Clark level ≥4, n (%)	63 (75.9)	16 (100)	0.037
Perineural invasion, Yes, n (%)	5 (6)	4 (22.2)	0.049
Nerve diameter ≥0.1 mm, n (%)	3 (3.6)	4 (22.2)	0.017
Vascular invasion, Yes, n (%)	1 (1.2)	1 (5.6)	NS
Desmoplasia, Yes, n (%)	1 (1.2)	3 (16.7)	0.02
Budding, Yes, n (%)	36 (42.9)	16 (88.9)	<0.01
Fibrosis burden, median (IQR)	0 (0;125)	155 (100;200)	<0.01
<i>Staging systems, n (%)</i>			
<i>TNM (AJCC-8)</i>			
pT1	33 (40.2)	4 (23.5)	0.02
pT2	19 (23.2)	1 (5.9)	
pT3	29 (35.4)	10 (58.8)	
pT4	1 (1.2)	2 (11.8)	
<i>TNM (Brigham)</i>			
1	32 (39.5)	3 (17.6)	NS
2a	38 (46.9)	8 (47.1)	
2b	9 (11.1)	4 (23.5)	
3	2 (2.5)	2 (11.8)	

AJCC-8 and Brigham's staging could not be performed in 3 and 4 cases, respectively due to missing values.

IQR: interquartile range.

variate analysis, as well as a strong correlation between the myxoid fibrotic pattern and the risk of metastasis in the multivariate analysis. The pattern of fibrosis may be relevant to the prognosis of epithelial tumours. In this regard, most oral SCC (OSCCs) exhibit two main patterns: "spindle" (arranged in rows of few cells around the neoplastic islands) and "network" (occupying the entire tumour stroma). The latter has apparently been linked to aggressive forms of OSCC (29, 30). Similarly, a myxoid reaction pattern, or so-called immature fibrotic reaction pattern, has been associated with bad prognoses in colorectal cancer (17, 18, 25, 26). Although a myxoid pattern surrounded by an intense inflammatory infiltrate can be found in NMSCC, we have observed that myxoid stromal changes in the invasive tumoural front, together with the absence of inflammatory cells, is highly specific for metastasizing cSCC. The relatively low sensitivity of this pattern in MSCC may be due to its presence in small, unnoticed areas. These foci may correspond to areas where a fibrotic/myxoid reaction inhibits the immune response ("immune response sanctuary"), thus favouring the metastatic process. We found this pattern to be strongly associated with budding, which is also linked to a higher metastatic risk (7, 8, 31). Both budding and a myxoid stroma are transitory phenotypes that appear in the tumour invasive front. CAFs-secreted TGFβ

may not only trigger EMT, but also induce an excess of type 1 collagen deposition, as observed in the keloidal pattern (25). These observations suggest that a mucopolysaccharide-rich microenvironment may play a role in favouring EMT (budding), as well as in blocking the host immunological response, and therefore increasing the metastatic risk.

We found areas of myxoid stroma to be easily detected by routine H&E staining in the advancing tumoural invasive front, even in poorly differentiated tumours. Conversely, we did not find α -SMA or fibronectin to increase the detection of this fibrotic pattern compared with H&E. Unlike previous studies, most areas of myxoid stroma in cSCC were devoid of α -SMA positivity, which may be due to several reasons: (i) fibrosis-inducing myofibroblasts are immature and do not express α -SMA; (ii) CAFs produce a mucopolysaccharide-rich stroma and thereby become nonessential; or (iii) myxoid-rich stroma is produced by a different cell.

In contrast to the myxoid pattern, we did not find any association between desmoplasia and metastatic risk in our series. Although there is some controversy about the definition of desmoplasia, many authors suggest that it confers tumoural growth and invasive advantages in cSCC (3, 19, 32). In the prospective study by Brantsch et al. (3), the local recurrence rate, but not the metastatic risk, was found to be higher in desmoplastic cSCC. In contrast, other authors have found this pattern to be associated with metastatic risk in cSCC (19, 24, 32). These heterogeneous results may reflect the lack of a common consensus in defining desmoplasia.

There are several limitations in our report that should be stated. First, there are potential errors due to the retrospective nature of our study. Second, all of the centers that participated in the study are reference university hospitals that are more likely to receive previously treated and aggressive tumours. This may account for the high number of recurrent tumours among MSCC samples in our series (20.4%).

In conclusion, we studied desmoplasia, the fibrotic burden and fibrosis patterns in a series of MSCC and NMSCC samples. Although fibrosis is a frequent finding in both aggressive and indolent tumours, our findings suggest that a myxoid pattern, together with an inflammatory exclusion (immature fibrotic pattern), is strongly associated with metastatic risk. Although it is perhaps premature to recommend the study of fibrotic patterns during routine examinations by pathologists, it is true that we all commonly observe that cSCC ending with small clusters or single tumoural cells, often surrounded by a stromal reaction, have a worse prognosis. This is due to the fact that these cells that can migrate and produce vascular or neural invasions. Our work has focused on this aspect and we have found that is not only the presence of isolated tumoural cells that increases the metastatic risk, also known as tumour budding, but also the microenvi-

ronment surrounding these cells that plays a role in bad prognoses. If our results are confirmed in further studies, the pattern of peritumoural fibrosis should be weighed as an additional factor to consider in histopathological assessments of cSCC with a prognostic value.

ACKNOWLEDGEMENT

This work has been supported by grant PI15/00236 from Fondo de Investigación Sanitaria (FIS), Fondo Europeo de Desarrollo Regional (FEDER), Instituto de Salud Carlos III, Ministerio de Sanidad, and the “Xarxa de Bancs de Tumours”.

REFERENCES

1. Alam M, Ratner D. Cutaneous squamous-cell carcinoma. *N Engl J Med* 2001; 344: 975–983.
2. Skulsky SL, O’Sullivan B, McArdle O, Leader M, Roche M, Conlon PJ, et al. Review of high-risk features of cutaneous squamous cell carcinoma and discrepancies between the American Joint Committee on Cancer and NCCN Clinical Practice Guidelines In Oncology. *Head Neck* 2017; 39: 578–594.
3. Brantsch KD, Meisner C, Schönfish B, Trilling B, Wehner-Caroli J, Röcken M, et al. Analysis of risk factors determining prognosis of cutaneous squamous-cell carcinoma: a prospective study. *Lancet Oncol* 2008; 9: 713–720.
4. Schmults CD, Karia PS, Carter JB, Han J, Qureshi AA. Factors predictive of recurrence and death from cutaneous squamous cell carcinoma: a 10-year, single-institution cohort study. *JAMA Dermatol* 2013; 149: 541–547.
5. Nieto MA, Huang RY-J, Jackson RA, Thiery JP. EMT: 2016. *Cell* 2016; 166: 21–45.
6. Toll A, Masferrer E, Hernández-Ruiz ME, Ferrandiz-Pulido C, Yébenes M, Jaka A, et al. Epithelial to mesenchymal transition markers are associated with an increased metastatic risk in primary cutaneous squamous cell carcinomas but are attenuated in lymph node metastases. *J Dermatol Sci* 2013; 72: 93–102.
7. Fujimoto M, Yamamoto Y, Matsuzaki I, Warigaya K, Iwahashi Y, Kojima F, et al. Tumor budding is an independent risk factor for lymph node metastasis in cutaneous squamous cell carcinoma: a single center retrospective study. *J Cutan Pathol* 2016; 43: 766–771.
8. Gonzalez-Guerrero M, Martínez-Cambor P, Vivanco B, Fernández-Vega I, Munquía-Calzada P, Gonzalez-Gutiérrez MP, et al. The adverse prognostic effect of tumor budding on the evolution of cutaneous head and neck squamous cell carcinoma. *J Am Acad Dermatol* 2017; 76: 1139–1145.
9. Nakanishi H, Oguri K, Takenaga K, Hosoda S, Okayama M. Differential fibrotic stromal responses of host tissue to low- and high-metastatic cloned Lewis lung carcinoma cells. *Lab Invest* 1994; 70: 324–332.
10. Ene-Obong A, Clear AJ, Watt J, Wang J, Fatah R, Riches JC, et al. Activated pancreatic stellate cells sequester CD8+ T cells to reduce their infiltration of the juxtatumoral compartment of pancreatic ductal adenocarcinoma. *Gastroenterology* 2013; 145: 1121–1132.
11. Watt J, Kocher HM. The desmoplastic stroma of pancreatic cancer is a barrier to immune cell infiltration. *Oncoimmunology* 2013; 2: e26788.
12. Liao D, Luo Y, Markowitz D, Xiang R, Reisfeld RA. Cancer associated fibroblasts promote tumor growth and metastasis by modulating the tumor immune microenvironment in a 4T1 murine breast cancer model. *PLoS One* 2009; 4: e7965.
13. Balsamo M, Scordamaglia F, Pietra G, Manzini C, Cantoni C, Boitano M, et al. Melanoma-associated fibroblasts modulate NK cell phenotype and antitumor cytotoxicity. *Proc Natl Acad Sci U S A* 2009; 106: 20847–20852.
14. Lagacé R, Grimaud JA, Schürch W, Seemayer TA. Myofibroblastic stromal reaction in carcinoma of the breast: variations of collagenous matrix and structural glycoproteins. *Virchows Arch A Pathol Anat Histopathol* 1985; 408: 49–59.
15. Lao XM, Liang YJ, Su YX, Zhang SE, Zhou X, Liao GQ. Distribution and significance of interstitial fibrosis and stroma-infiltrating B cells in tongue squamous cell carcinoma. *Oncol Lett* 2016; 11: 2027–2034.
16. Clapéron A, Mergey M, Aoudjehane L, Ho-Boulidoires TH, Wendum D, Prignon A, et al. Hepatic myofibroblasts promote the progression of human cholangiocarcinoma through activation of epidermal growth factor receptor. *Hepatology* 2013; 58:2001–2011.
17. Ueno H, Jones AM, Wilkinson KH, Jass JR, Talbot IC. Histological categorisation of fibrotic cancer stroma in advanced rectal cancer. *Gut* 2004; 53: 581–586.
18. Ueno H, Shinto E, Kajiwara Y, Fukazawa S, Shimazaki H, Yamamoto J, et al. Histologic Categorization of Desmoplastic Reaction: Its Relevance to the Colorectal Cancer Microenvironment and Prognosis. *Ann Surg Oncol* 2015; 22: 1504–1512.
19. Breuninger H, Schaumburg-Lever G, Holzschuh J, Horny HP. Desmoplastic squamous cell carcinoma of skin and vermilion surface: a highly malignant subtype of skin cancer. *Cancer* 1997; 79: 915–919.
20. NCCN Clinical Practice Guidelines in Oncology (NCCN Guidelines®) Squamous Cell Skin Cancer 1.2017. National Comprehensive Cancer Network, Inc.; 2016. Available at: <http://NCCN.org>. Accessed July 1, 2017.
21. Stratigos A, Garbe C, Lebbe C, Malvey J, del Marmol V, Pehamberger H, et al. Diagnosis and treatment of invasive squamous cell carcinoma of the skin: European consensus-based interdisciplinary guideline. *Eur J Cancer* 2015; 51: 1989–2007.
22. Jambusaria-Pahlajani A, Kanetsky PA, Karia PS, Hwang WT, Gelfand JM, Whalen FM, et al. Evaluation of AJCC tumor staging for cutaneous squamous cell carcinoma and a proposed alternative tumor staging system. *JAMA Dermatology* 2013; 149: 402–410.
23. Edge S, Byrd DR, Compton CC, Fritz AG, Greene FL, Trotti A. AJCC cancer staging manual. 7th ed. New York: Springer.
24. Gonzalez-Guerrero M, Martínez-Cambor P, Vivanco B, Fernández-Vega I, Munquía-Calzada P, González-Gutiérrez MP, et al. The adverse prognostic effect of tumor budding on the evolution of cutaneous head and neck squamous cell carcinoma. *J Am Acad Dermatol* 2017; 76: 1139–1145.
25. Ueno H, Jones A, Jass JR, Talbot IC. Clinicopathological significance of the “keloid-like” collagen and myxoid stroma in advanced rectal cancer. *Histopathology* 2002; 40: 327–334.
26. Ueno H, Shinto E, Hashiguchi Y, Shimazaki H, Kajiwara Y, Sueyama T, et al. In rectal cancer, the type of desmoplastic response after preoperative chemoradiotherapy is associated with prognosis. *Virchows Arch* 2015; 466: 655–663.
27. Tsujino T, Seshimo I, Yamamoto H, Ngan CY, Ezumi K, Takemasa I, et al. Stromal myofibroblasts predict disease recurrence for colorectal cancer. *Clin Cancer Res* 2007; 13: 2082–2090.
28. Watt J, Kocher HM. The desmoplastic stroma of pancreatic cancer is a barrier to immune cell infiltration. *Oncoimmunology* 2013; 2: e26788.
29. Seifi S, Shafaei S, Shafiq E, Sahabi SM, Ghasemi H. Myofibroblast stromal presence and distribution in squamous epithelial carcinomas, oral dysplasia and hyperkeratosis. *Asian Pac J Cancer Prev* 2010; 11: 359–364.
30. Kawashiri S, Tanaka A, Noguchi N, Hase T, Nakaya H, Ohara T, et al. Significance of stromal desmoplasia and myofibroblast appearance at the invasive front in squamous cell carcinoma of the oral cavity. *Head Neck* 2009; 31: 1346–1353.
31. Agar NJM, Kirton C, Patel RS, Martin RCW, Angelo N, Emanuel PO. Predicting lymph node metastases in cutaneous squamous cell carcinoma: Use of a morphological scoring system. *N Z Med J* 2015; 128: 59–67.
32. Breuninger H, Brantsch K, Eigentler T, Häfner HM. Comparison and evaluation of the current staging of cutaneous carcinomas. *J Dtsch Dermatol Ges* 2012; 10: 579–586.